JANE Optimisation of a novel hot air contactless single incremental point forming of polymers

Almadani, M., Guner, A., Hassanin, H. and Essa, K.

Mohammad Almadani, Ahmet Guner, Hany Hassanin, Khamis Essa, Optimisation of a novel hot air contactless single incremental point forming of polymers, Journal of Manufacturing Processes, Volume 117, 2024, Pages 302-314, ISSN 1526-6125, https://doi.org/10.1016/j.jmapro.2024.02.042.

Journal of Manufacturing Processes 117 (2024) 302–314

Contents lists available at ScienceDirect

Journal of Manufacturing Processes

journal homepage: www.elsevier.com/locate/manpro

Optimisation of a novel hot air contactless single incremental point forming of polymers

Mohammad Almadani [a,b], Ahmet Guner [a], Hany Hassanin [c,*], Khamis Essa [a,*]

[a] Mechanical Engineering, University of Birmingham, Edgbaston, Birmingham B15 2TT, UK
[b] Department of Mechanical Engineering Technology, Yanbu Industrial College, Yanbu Al-Sinaiyah City 41912, Saudi Arabia
[c] School of Engineering, Technology, and Design, Canterbury Christ Church University, B15 2TT, UK

ARTICLE INFO

Keywords:
Sheet forming
Response surface methodology
Contactless incremental forming
Formability
Design of experiment

ABSTRACT

This study presents a new contactless sheet forming method that utilises hot air as a forming tool to address tool wear challenges in single-point incremental forming. Experiments were conducted on a 3-axis CNC machine equipped with a hot air nozzle on a polycarbonate sheet. A design of experiment (DOE) approach was employed, evaluating five control factors: air pressure, air temperature, feed rate, tool offset, and step down. The evaluation criteria for the formed sheets are profile variation, thickness variation, and surface roughness. The results indicate that air temperature and feed rate have the most significant influence on the deformation process. Additionally, air pressure and feed rate substantially impact both thickness variation and surface roughness of the formed material. To optimise the process parameters for high-quality forming, a prediction model is developed. The optimised process shows good agreement with the predicted model regarding profile and thickness variations. However, it does not align with surface roughness due to the stepwise nature and inherent waviness of the contactless forming technique. This study offers a promising approach for developing innovative contactless forming techniques using hot pressurised air as a forming tool. The proposed technique has the potential to significantly reduce tool wear and lubrication requirements.

1. Introduction

Single Point Incremental Forming (SPIF) is an efficient and versatile alternative to conventional forming techniques, particularly for low-volume batches, prototypes, and specialised parts. Unlike traditional forming methods, SPIF doesn't necessitate expensive or specialised tools. Instead, a rigid tool follows a series of planar shapes or a single spiral contour to create parts. This recent process has unlocked new possibilities for sheet forming, eliminating the need for a specific die. It's a manufacturing technique that employs a customisable tool to shape sheets into specific configurations. Through the utilisation of computer numerically controlled (CNC) technology, SPIF can achieve high precision and accuracy, allowing for the creation of complex shapes with minimal lead time and low forming forces. These advantages make SPIF an exceptionally adaptable and flexible manufacturing process that harmonises with the demands of Industry 4.0 [1–3].

In the aerospace industry, SPIF is employed to manufacture lightweight components with intricate shapes, including aircraft panels and engine components. SPIF offers the advantage of reducing material waste while ensuring high precision, rendering it a highly suitable manufacturing process for the aerospace industry [4,5]. The automotive industry also reaps the benefits of SPIF, particularly in the production of low-volume components with complex geometries, like exhaust systems and car body parts. SPIF's capability to achieve high formability with minimal tooling costs positions it as an ideal solution for the automotive industry [6–8]. In the biomedical industry, SPIF has found application in the manufacturing of implants, including orthopedic implants and dental prostheses. SPIF's precise and customisable forming capabilities have rendered it an appealing alternative to traditional manufacturing processes [9].

The single-point incremental forming process has garnered researchers' attention for improving its forming results and eliminating defects. Several investigations have focused on the process elements that significantly impact the performance of Single Point Incremental Forming (SPIF). These factors include the thickness of the sheet, the depth of vertical steps, the size and speed of the forming tool, the use of lubrication, and the quality of the material. For instance, a study by Kim et al. found that using a roller end tool provides better formability than a

* Corresponding authors.
E-mail addresses: hany.hassanin@canterbury.ac.uk (H. Hassanin), k.e.a.essa@bham.ac.uk (K. Essa).

https://doi.org/10.1016/j.jmapro.2024.02.042
Received 23 June 2023; Received in revised form 24 September 2023; Accepted 19 February 2024
Available online 14 March 2024

hemispherical tool when deforming an aluminum alloy sheet [4]. Meanwhile, another study by Azevedo et al. investigated the effects of lubricants on the surface finish of steel (DP780) and aluminum (AA1050-T4) sheets [5]. The authors applied various types of lubricants, including Total Finaro LB5746, Repsol SAE 30, Moly Slip AS 40, Moly Slip HSB, and Weicon AL-M. The study demonstrated that selecting the appropriate lubricant viscosity depends on the hardness of the material being formed to achieve optimal performance. The findings indicated that SAE 30 lubricant produced a smoother surface finish when applied to AA1050-T4, while AS-40 grease resulted in a rougher surface finish. Conversely, AS-40 grease provided a smoother surface finish for steel, while SAE-30 gave a rougher surface finish. Consequently, low-viscosity lubricant is needed for materials with high hardness, whereas high-viscosity lubricant is necessary for materials with low hardness.

While the SPIF process was initially developed for metal materials, it has also been applied to polymeric sheets, thermoplastics, and composite materials. The SPIF process for polymers is a cost-effective method for producing customised product parts from a wide range of materials, including metals, polymers, and composites [10]. The process has been refined over the years through research focused on factors such as sheet thickness, tool size, lubrication, and material properties [11]. The material properties of polymers play a crucial role in determining their suitability for the SPIF process, with factors such as ductility and color stability impacting the final product's quality. However, achieving successful polymer material formation requires a thorough understanding of these properties. To address this, Martins et al. [8] conducted a comprehensive study to assess the formability of five different types of polymers using SPIF. The study utilised a rigid tool with diameters of 10 and 15 mm and sheet thicknesses of 2 and 3 mm. Each polymer material exhibited unique properties that influenced its suitability for SPIF. For instance, PE and PA showed higher ductility, making them suitable for components with significant wall angles. Conversely, PVC displayed lower springback, making it the ideal choice when high accuracy is required. PC proved excellent for applications demanding high surface quality, as it retained its color during the incremental cold forming technique. However, POM performed the poorest among all the investigated polymers due to its limited ductility. Additionally, the study revealed color changes in the polymer materials after the SPIF process, emphasising the importance of considering color stability when selecting the polymer material for the process.

The SPIF process is influenced by several parameters, including tool size, step size, feed rate, and spindle speed, all of which can significantly impact the final shape of the polymer sheet. A study by Le et al. [12] on the effects of these parameters on forming polypropylene sheets revealed that using a small tool radius reduces the formability of the polypropylene sheet, while an increase in step size decreases the formability and can lead to defects such as final shape wrinkles. The study also found that elevating the spindle speed of the tool increases formability, and using high spindle speeds with small step sizes and large tool sizes can further improve the formability rate of PP sheets. However, despite the success in optimising these parameters, the rigid tool used in SPIF can still lead to several drawbacks and needs to be eliminated from the process. In addition to the effects of traditional SPIF parameters, alternative tools have been explored to improve the process. For example, Jurisevic et al. [13] have suggested using a waterjet nozzle instead of a rigid tool. In their study, it was found that the surface finish of the sheet was notably smoother, and no wear was detected on the tool. Moreover, the equipment cost was considerably lower, and the entire process was deemed to have a more environmentally friendly impact. The use of a waterjet nozzle was successful in deforming a brass sheet, and the accuracy, energy efficiency, and forming time were better than those achieved with conventional methods. To achieve the best possible results, the researchers conducted a thorough examination of various parameters such as water pressure, stand-off distance, nozzle geometry, and forces at the interface of the tool and the workpiece. After careful analysis, they made necessary adjustments to these parameters to optimise the process [13,14].

Design of Experiments (DOE) and statistical analysis have been established as effective methods for studying the influence of operating parameters on sheet forming processes. These techniques have been proven to be particularly useful in understanding the effects of various parameters on the forming process, which, in turn, helps optimise the process for superior performance. Statistical methods can provide valuable insights into the process, including identifying the most significant parameters, evaluating the effect of interactions between parameters, and predicting optimal settings for improved performance. Therefore, the use of DOE and statistical analysis has become increasingly popular in various manufacturing processes to enhance the quality of the final product while minimising the cost and time required for production. Yang et al. [15] employed the Taguchi approach to ascertain the optimal working parameters for cutting glass fiber, while Bacchewar et al. [16] utilised response surface Design of Experiments (DOE) and ANOVA methodologies to analyse the pertinent process variables in selective laser sintering. Similarly, Hussain et al. [17] Ham and Jeswiet [18] and Filice et al. [19] all employed DOE methodologies to study the influence of processing parameters, including feed rate, rotational speed, and sheet thickness, on formability in incremental sheet forming.

Ham and Jeswiet [20] conducted two Design of Experiments (DOEs) to identify key factors affecting the SPIF process to achieve effective deformation without defects like tears or cracks. They investigated how these key variables influenced the process's formability. In another study, Ambrogio et al. [21] employed a modeling approach to link process parameters to geometrical inaccuracies in SPIF using statistical analytical techniques, including DOE and ANOVA. Similarly, Essa and Hartley [10] utilised DOE to optimise process parameters for both sheet metal spinning and single-point incremental forming [17]. Majagi and Chandramohan [11] employed a Box-Behnken experimental design and response surface methodology to assess the effects of speed, feed rate, and coolant on the surface roughness, thickness reduction, and hardness of aluminum sheets Furthermore, Elgahwail et al. [22] used response surface DOE and analysis of variance to determine optimal process parameters for the MPF process, particularly regarding springback amount. These studies collectively demonstrate that DOE and statistical analysis are effective tools for identifying and optimising critical process parameters in various sheet forming processes, including cutting glass fiber, selective laser sintering, sheet metal spinning, and incremental sheet forming.

The SPIF process for polymers still encounters challenges such as issues with geometric precision, thickness variation, wrinkling, and rough surface finishes. These issues arise due to the physical interaction between the tool and the polymer sheet [7]. To address these challenges, this study introduces and optimises a novel SPIF process by employing hot compressed air as the shaping tool, completely eliminating physical contact between the tool and the polymer sheet. The proposed process, dubbed Contactless Single Point Incremental Forming (CSPIF), is not only eliminates the need for a rigid tool but also results in substantial cost savings. It reduces process costs by lowering tool expenses and mitigating factors such as tool wear, all while eliminating the necessity for lubrication. Furthermore, this approach enhances surface finish by avoiding direct contact, and it improves the shaping of less malleable polymer materials. This enhancement extends to quality aspects related to springback and geometric precision. Since this deformation process involves no friction forces, there is no risk of wrinkling or twisting. In this research, the process was developed and optimised using Design of Experiments (DOE) to address the geometric defects commonly encountered in the SPIF process for polymers. The primary focus was on identifying the most suitable combination of various parameters to enhance the final product's quality. The study employed DOE techniques to identify key parameters and their impact on profile variation, thickness variation, and surface roughness during the production of a truncated pyramid. The research also determined the ideal operating parameter settings for achieving the best quality features using a min-

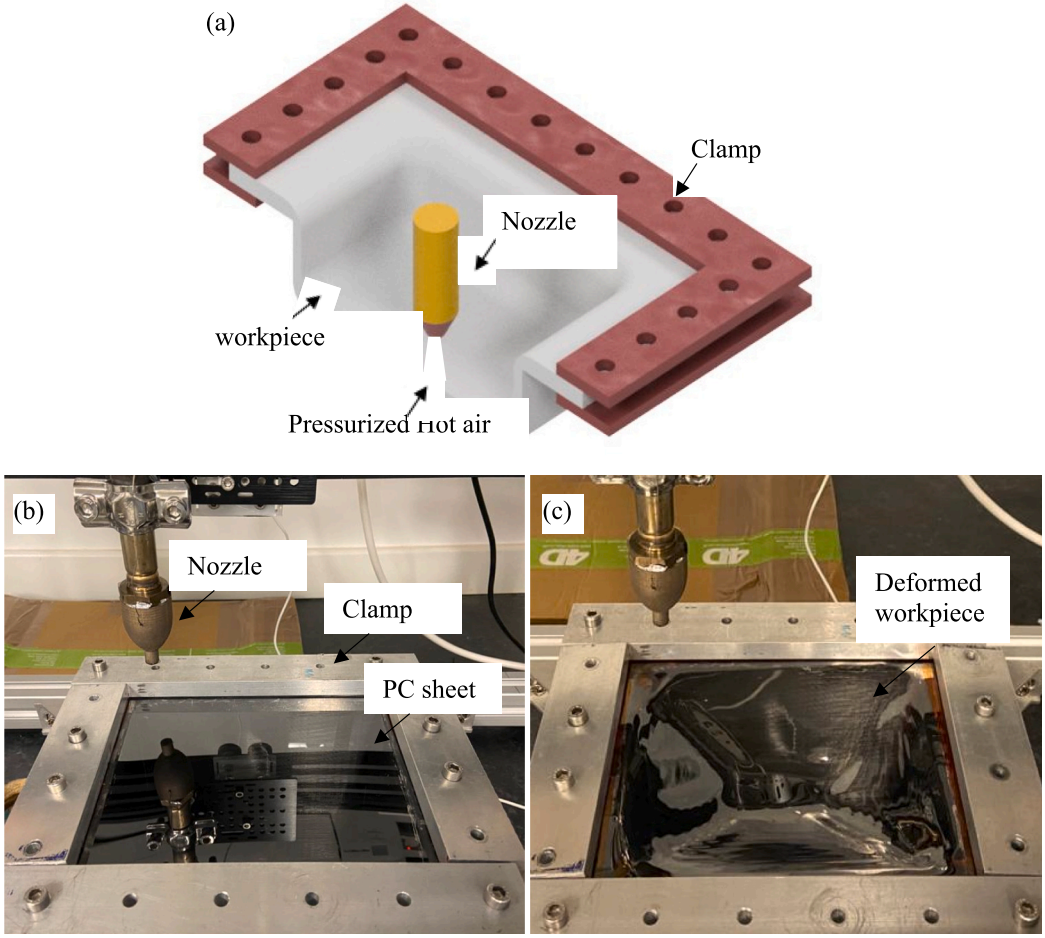

Fig. 1. (a) A schematic of the process, (b) the experimental setup before forming, (c) after deformation. A video of the process: https://cccu-my.sharepoint.com/:v:/g/personal/hh36_canterbury_ac_uk/EY4dqyhotrVJomEFsv1JP94B1DUkkwWKT75Zeqpg-J00mg?e=5VIkT3

max optimization method.

2. Method and experimental

The CSPIF process is a sheet-forming technique that involves the gradual deformation of a sheet workpiece using a non-contact heated compressed air tool. This process employs pressurised hot air instead of a solid tool. The designed setup comprises essential components, including a nozzle, an in-line air and gas heater pipe, a temperature controller, an air compressor, an air tube, and an integrated computer numerical control system with a clamped frame. The nozzle is a crucial part of the setup and controls the flow of hot pressurised air, producing a force on the polymer material while avoiding direct contact. The nozzle was designed using SolidWorks, and a metal laser powder bed fusion printer was used to produce the alloy steel nozzle. The design allows for the measurement and management of the temperature and pressure of the hot air at the inlet of the nozzle. The contactless process is illustrated in Fig. 1a through the schematic diagram shown. It depicts the various components and their interactions during the process. Fig. 1b depicts the setup before forming, while Fig. 1c shows the setup after the forming stage.

The mechanics of this process closely resemble those of conventional SPIF, with the key difference being that the deformation is applied to the sheet using a contactless hot compressed air tool, thus eliminating friction. The process begins by securing the polycarbonate sheet at its edges to prevent uncontrolled distortions. The contactless tool is mounted on a 3D printer machine, which controls the tool's movement through CNC programming and G-code-defined paths, as seen in Fig. 2a. The force of the deformation is generated by adjusting the air pressure, regulated by the air compressor, and the air temperature, which is controlled by a PID temperature controller. The deformation process was initiated by positioning the nozzle at its initial location with a predetermined gap, as programmed in the G-code of the 3D printer machine, as illustrated in Fig. 2b,c. Subsequently, the nozzle began to follow the predefined path outlined in the G-code.

In this study, this path assumed a truncated pyramid shape, as shown in Fig. 3. Initially, as can be seen in Fig. 2c, the nozzle moved along the -z axis at a specific feed rate and distance of 152 mm, and then proceeded to move along the -x axis with a specific feed rate and distance of 120 mm, forming a rectangular shape. Upon completing this initial trajectory, the nozzle descended along both the -x and -z axes, before shifting along the -y axis with a specified step-down gap to initiate the second path. This process continued until the final path was attained, covering an area of 62 × 30 mm^2. The step-down between each step was set to range between 0.5, 0.75, and 1 mm, in a total depth of 5, 7.5, and 10 mm.

Five distinct parameters were identified as the main key factors influencing the final geometrical features. These parameters include air pressure, air temperature, feed rate, the initial gap between the nozzle and the polymer sheet, and step-down thickness. The air pressure and temperature are critical parameters that are controlled using an air heater and controller. The air compressor is used to deliver pressurised air through a plastic hose, which is connected to the air heater on one end and the air compressor on the other. The compressed air is heated to the required temperature as it passes through the heating element in the heater. After reaching the desired temperature, the heated compressed

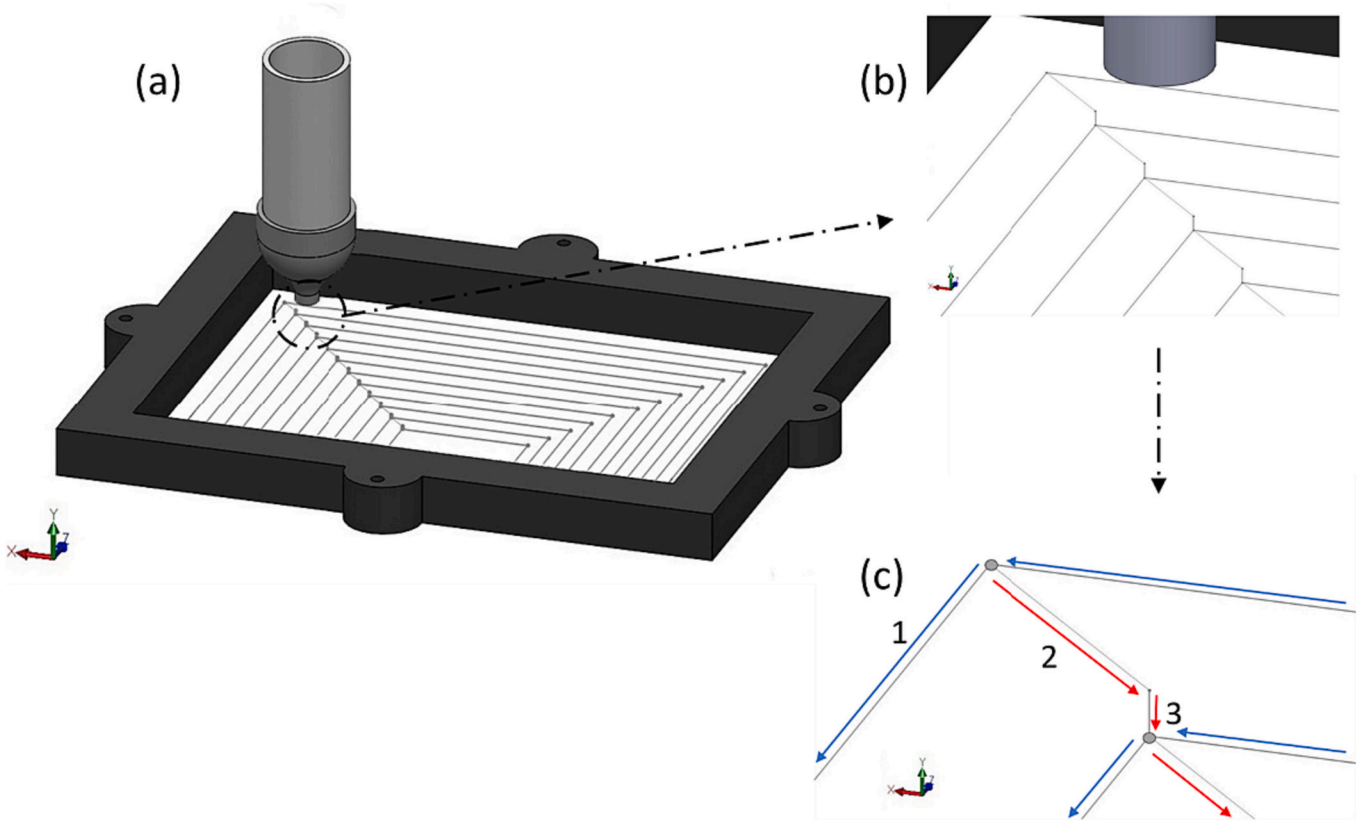

Fig. 2. The nozzle trajectory a) Completed path, b) location of the nozzle over the sheet, and c) Movement along the path.

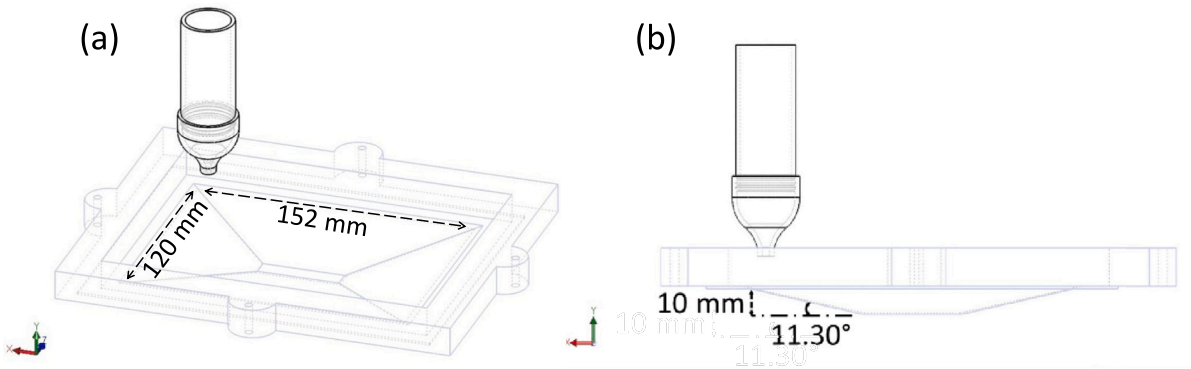

Fig. 3. The final Shape geometry a) 3d view, b) Side view.

Table 1
Properties of the Lexan® 9030 polycarbonate (PC) sheet.

Thickness	0.75 (mm)
Density	1.2 (g/cm)
Young's modulus	2.3 (Gpa)
Yield stress	60 (Mpa)
Poisson's Ratio	0.38
Maximum elongation	110 (%)
Thermal conductivity	0.2 (W/m.°C)

air is directed to the nozzle, located at the exit of the heater. The nozzle is an essential component of the process, as it increases the air velocity, enhancing the forming force and pressure concentration in a specific area of the polycarbonate sheet. The nozzle speed, the distance between the nozzle and the polymer sheet, and step-down thickness are also crucial parameters carefully controlled to achieve the desired result.

The process begins with the startup of the air heater and the temperature adjustment set by the controller. Temperature adjustment is critical as it determines the heating temperature of the compressed air, which is essential for the successful deformation of the polymer sheet. Once the temperature is set, the air compressor is started, and the pressurised air is delivered through the plastic hose to the air heater with a certian pressure that is adjusted using the regulator. The nozzle has been specifically designed to incorporate a thermocouple, facilitating precise measurement of the high-temperature compressed air passing through it. Additionally, a thermal camera was utilised to visualise and analyse the temperature distribution within the nozzle.

For this study, a Lexan® 9030 workpiece made of polycarbonate

Table 2
Propose control factors and their levels.

Factor	Parameter	Level 1	Level 2	Level 3
A	Air pressure	0.75 (bar)	1 (bar)	1.25 (bar)
B	Air temperature	140 (°C)	160 (°C)	180 (°C)
C	Feed rate	500 (mm/min)	750 (mm/min)	1000 (mm/min)
D	Tool offset	4 (mm)	6 (mm)	8 (mm)
E	Step down	0.5 (mm)	0.75 (mm)	1 (mm)

(PC) sheet, measuring 170 mm by 205 mm and with a thickness of 0.75 mm, was selected. The material properties of the PC sheet are outlined in Table 1. To obtain a comprehensive understanding of the PC sheet's behavior at different temperatures, stress and strain curves were analysed at elevated temperatures. These curves illustrate the relationship between temperature and the mechanical properties of PC sheets and were obtained from previous research as low-strain rate of tensile test curves [23].

The commercial software Minitab 20 was chosen as the analytical tool for this study because it is a powerful statistical software package widely used in the industry for data analysis. The purpose of the Design of Experiments (DOE) was to evaluate the effects of the experimental factors on profile variation, thickness variation, and surface roughness, which are crucial parameters in the manufacturing process. These factors included air pressure, air temperature, feed rate, tool offset, and step down, which were chosen based on their relevance to the conventional SPIF manufacturing process and their association with the new tool. Furthermore, new parameters were introduced to complement the new hot compressed air tool, which were tested and selected for their potential impact on the product's quality.

The primary objective of this study was to develop an empirical model capable of predicting the responses of the aforementioned experimental factors for any combination of operating conditions. By doing so, the model could aid in the optimisation of the novel contactless SPIF manufacturing process and the production of a high-quality end product. To achieve this goal, a response surface design was employed to construct a series of experiments using only the five selected components. This approach allowed for a more detailed analysis of the interaction between the various factors, identification of the optimal levels for each factor, and their impact on the product's quality.

In this Design of Experiments (DOE), quantitative quality parameters included variances in profile, thickness, and surface roughness, were utilised as critical factors in determining the overall quality of the formed sheet. To measure the average surface roughness (Ra) of each part, a Mitutoyo Formtracer Avant S-3000 Model Surface Roughness Tester was employed. The coordinate measurement machine (CMM) was used to measure the profile and thickness of the pyramid across the entire cross-section of each experiment. Eq. (1) was utilised to calculate the profile and thickness variation of the deformed parts [22].

$$\text{Thickness variation} = \sqrt{\frac{1}{N}\sum_{i=1}^{N}(xi - \bar{x})^2} \quad (1)$$

Here, N represents the number of points where the workpiece thickness was measured, xi is the thickness at a given point i, and $\bar{x}$ is the average thickness value for all points.

Three levels of the method were used to generate data. The levels of factor control are presented in detail in Table 2, providing information about the high, medium, and low levels of the SPIF contactless process parameters. To create the truncated pyramid-shaped product, a total of 54 trials were conducted using the experimental surface response method's design.

To analyse the compressed air pressure and temperature distributions and values produced by the nozzle design in the contactless SPIF process, a Computational Fluid Dynamics (CFD) model was created using ANSYS Fluent software. The model consisted of a reducer, a sheet, and a closed environmental box. The reducer had a 33 mm inlet diameter, a 5 mm outlet diameter, and a height of 55 mm to control the pressure and temperature of the air flowing out from the heater. A polycarbonate sheet was included in the simulation under the nozzle outlet, positioned 6 mm away from the reducer nozzle, to model a deformed sheet and predict the pressure and temperature values on the surface of the sheet during the forming process.

A hybrid mesh was created using a combination of structured and unstructured meshing techniques, with a fine inflation mesh of 5 layers in regions of high flow complexity, as shown in Fig. 4. The k-ε model was employed to simulate turbulent flows, with the SIMPLC algorithm used in the simulation to provide accurate and reliable results while minimising computational costs. In the simulation, time step increments were set to be steady, meaning that the time between each step remained constant throughout the simulation.

3. Results and discussions

3.1. DoE results

The measured findings for the variations in profile, thickness, and surface roughness from 54 experiments are presented in Table 3. The table reveals that using trial 22 produced the lowest profile variation of 0.48 mm, whereas trial 50 yielded the lowest thickness variation of 0.04 mm, Additionally, trial 39 resulted the lowest surface roughness of 0.15 μm.

The calculated *P*-value is a statistical measure that indicates the probability of obtaining an observed effect due to chance alone in the context of hypothesis testing. A commonly accepted criterion for statistical significance is a P-value of 0.05 or less. This indicates that the

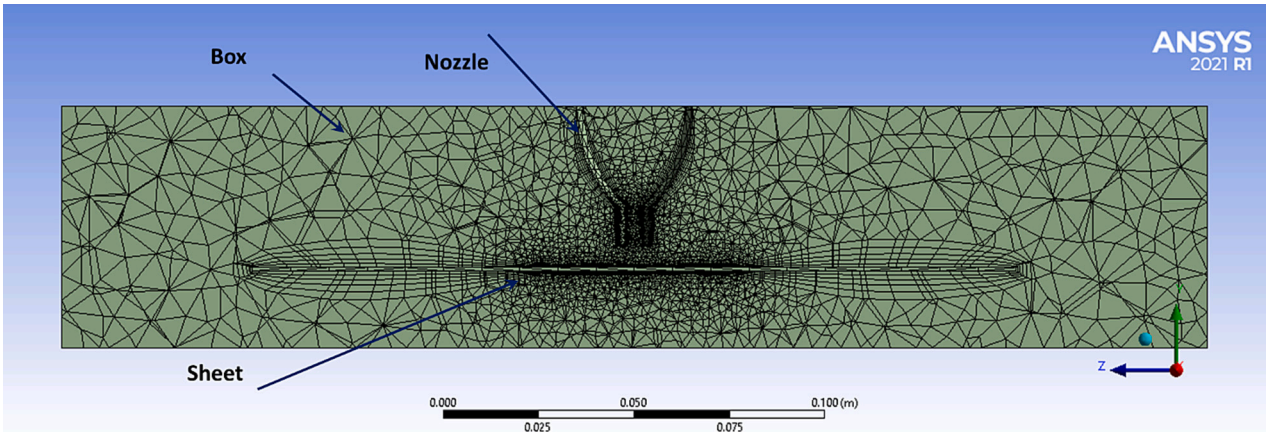

Fig. 4. Mesh of the CFD model.

Table 3
The surface response design and measured results.

Run	Air pressure (bar)	Air temp. (°C)	Feed rate (mm/min)	Tool offset (mm)	Step down (mm)	Profile variation (mm)	Thickness variation (mm)	Surface roughness (Ra) μm
1	1.25	140	1000	8	0.5	1.18	0.08	0.25
2	1.25	140	1000	4	0.5	1.37	0.11	0.30
3	1.25	140	500	4	1	2.92	0.27	0.59
4	1.25	140	1000	4	1	2.92	0.10	0.23
5	1.25	180	1000	8	1	1.07	0.12	0.23
6	0.75	140	500	8	0.5	2.88	0.15	0.79
7	1.25	180	1000	4	0.5	0.94	0.07	0.42
8	1	160	750	6	0.75	1.35	0.06	0.16
9	0.75	180	500	8	1	2.39	0.37	0.81
10	1.25	140	500	4	0.5	4.42	0.44	0.38
11	0.75	180	1000	4	0.5	1.40	0.13	0.23
12	0.75	140	1000	8	1	1.64	0.17	0.47
13	0.75	140	500	4	1	1.56	0.27	0.90
14	1.25	180	500	4	1	0.75	0.07	0.38
15	0.75	180	500	8	0.5	3.12	0.28	0.62
16	0.75	180	500	4	0.5	2.83	1.01	0.80
17	0.75	140	500	8	1	3.53	0.48	0.39
18	1.25	180	1000	4	1	2.26	0.07	0.28
19	1	160	750	6	0.75	1.35	0.06	0.16
20	0.75	180	1000	8	0.5	1.54	0.10	0.35
21	1.25	140	1000	8	1	1.11	0.09	0.33
22	1.25	180	500	8	1	0.48	0.10	0.30
23	1.25	180	1000	8	0.5	0.97	0.07	0.34
24	0.75	180	1000	8	1	1.00	0.15	0.17
25	0.75	140	500	4	0.5	4.15	0.18	0.53
26	0.75	140	1000	4	1	2.03	0.07	0.88
27	1	160	750	6	0.75	1.35	0.06	0.15
28	1	160	750	6	0.75	1.35	0.06	0.16
29	1	160	750	6	0.75	1.35	0.06	0.15
30	0.75	180	500	4	1	1.49	0.33	0.99
31	1	160	750	6	0.75	1.35	0.06	0.15
32	1.25	180	500	8	0.5	0.75	0.12	0.29
33	1.25	140	500	8	0.5	4.17	0.41	0.35
34	0.75	140	1000	8	0.5	1.60	0.14	0.37
35	0.75	140	1000	4	0.5	2.38	0.14	0.38
36	1.25	180	500	4	0.5	1.78	0.17	0.25
37	0.75	180	1000	4	1	1.93	0.19	0.61
38	1.25	140	500	8	1	2.28	0.20	0.63
39	1	160	750	6	0.75	1.35	0.06	0.15
40	1	160	750	6	0.75	1.35	0.06	0.15
41	1	160	750	8	0.75	1.33	0.05	0.36
42	1	140	750	6	0.75	3.49	0.22	0.91
43	1	160	750	6	0.75	1.35	0.06	0.16
44	1.25	160	750	6	0.75	2.73	0.23	0.39
45	1	160	750	6	0.75	1.35	0.06	0.16
46	1	160	500	6	0.75	2.17	0.17	0.46
47	1	160	750	6	0.75	1.35	0.06	0.15
48	1	160	1000	6	0.75	1.57	0.06	0.37
49	1	180	750	6	0.75	4.21	0.39	0.47
50	1	160	750	4	0.75	1.17	0.04	0.30
51	1	160	750	6	0.5	0.53	0.07	0.38
52	0.75	160	750	6	0.75	3.59	0.34	0.37
53	1	160	750	6	1	1.80	0.06	0.41
54	1	160	750	6	0.75	1.35	0.06	0.15

observed effect is highly unlikely to be a result of chance and instead suggests a strong correlation between the variables being tested [24,25].

In this study, the P-values of the important factors and their interactions were calculated and are presented in Table 3. Factors with *P*-values less than or equal to 0.05 were considered statistically significant, indicating their influence on the response. These results were then used to develop a predictive model that can aid in optimising the process parameters and ensuring high-quality products.

Table 3 presents the results of an experiment on the impact of various parameters on the forming process. The data clearly shows that the forming feed rate is a significant factor affecting profile variation, thickness variation, and surface roughness. Additionally, air pressure also significantly impacts thickness variation and surface roughness. However, the impact of air pressure on profile variation is not significant. The air temperature of the pressurised air is also an important factor that affecting profile variation, but its impact on the thickness variation and surface roughness is not significant.

Interestingly, the interactions between various parameters also have a significant impact on the forming process. Specifically, the interaction between air pressure and air temperature, air temperature and feed rate, and feed rate and step-down all have a significant impact on the product's profile variation. The thickness variation is also significantly affected by the interaction between air pressure and temperature (Table 4).

3.2. *Profile variation*

The thermocouple recorded the measured temperature, while the RS T-10 smart camera was utilised to monitor the temperature distribution during the deformation process. Fig. 5a and the accompanying video

Table 4
The *P*-values of the important factors and interactions.

	Profile variation	Thickness variation	Surface roughness (Ra)
Air pressure (A)	–	0.01403	0.00020
Air temperature (B)	0.00027	–	–
Feed rate (C)	0.00026	0.00007	0.00086
Tool offset (D)	–	–	–
Step down (E)	–	–	–
Important interactions	(A*B) 0.04523 (B*C) 0.01280 (C*E) 0.00285	(A*B) 0.00802	–

show a recording from the thermal camera during the forming process. Additionally, the significance of air temperature during the DOE study is depicted in Fig. 5b, which presents a typical parabolic curve representing the effect of air temperature on profile variation. The data revealed that the minimum profile variation was achieved at a temperature near 160 °C. Deviation in profile variation increased when the temperature exceeded or fell below 160 °C.

If the air temperature during the forming of the PC sheet is less than 160 °C, it affects the sheet deformation, causing the total deformation to be less than the target profile. The pressure applied at the same temperature to the nozzle may not be sufficient to deform the sheet properly. Similarly, an increase in the profile variation was also observed at temperatures higher than 160 °C, as the sheet becomes overly deformed due to the exposure to higher temperatures.

The lowest profile variation and closest match to the CAD drawing were achieved at the smallest valley of the U-shaped curve around 160 °C. This indicates that the profile is more uniform at this temperature, making it the optimum air temperature to deform the polycarbonate sheet to reach the target profile.

In Fig. 5c, the profile of the deformed polycarbonate sheet is shown at different air temperatures, including 140 °C, 160 °C, and 180 °C, alongside the CAD drawing. At 140 °C, a significant profile variation is observed. However, when the temperature is increased to 160 °C, a significant reduction in the profile variation becomes more apparent. This is due to the glass transition temperature of the polycarbonate, which is approximately 156.15 °C. Beyond this temperature, the material becomes more pliable and gradually softens. At around 160 °C, the material reaches a critical point where it can begin to flow and take on new shapes. This explains why the profile variation was at its minimum at this temperature [26,27].

Furthermore, the storage modulus of the polycarbonate, which stores energy elastically and resists deformation, is higher until it reaches 150 °C and decreases to zero at around 160 °C [28]. However, at higher temperatures, such as 180 °C, the material becomes overly softened, resulting in an increase in deformation. At 160 °C, the profile variation closely matches the CAD drawing, indicating that the profile is more uniform. Therefore, the optimum air temperature to deform the polycarbonate sheet and achieve the target profile was recorded around 160 °C. Moreover, it's worth noting that the workpiece did not exhibit any signs of degradation after the deformation process. Additionally, thermoplastic materials have the ability to be heated up to their glass transition temperature and then cooled down to room temperature

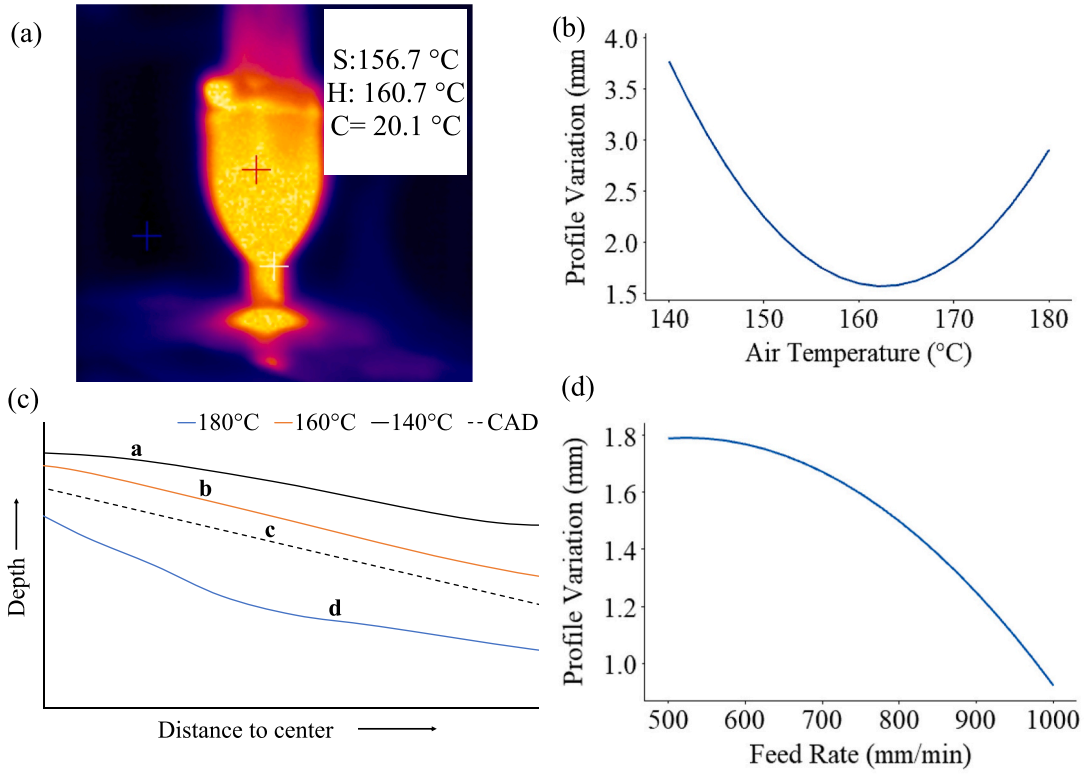

Fig. 5. (a) One of the thermal camera snapshot showing temperature distribution (b) Effect of compressed air temperature on Profile variation using (a) DoE results, (c) measured profile, (d) effect of federate on the profile variation. Video of the thermal camera during forming https://cccu-my.sharepoint.com/:v:/g/personal/hh36_canterbury_ac_uk/ESqLkdbfnK1Fj9mhJXSK970BoHP6xlsfXtzTbzaS7f1ARA?e=xvfDhX

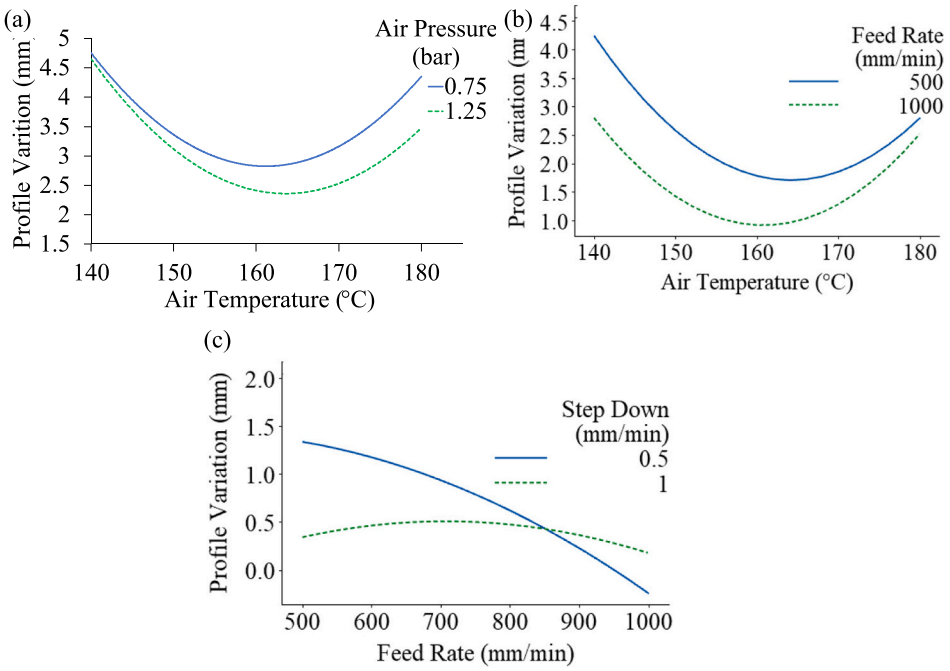

Fig. 6. Effect on profile variation of interactions between (a) air pressure and air temperature (b) air temperature and feed rate (c) feed rate and step down.

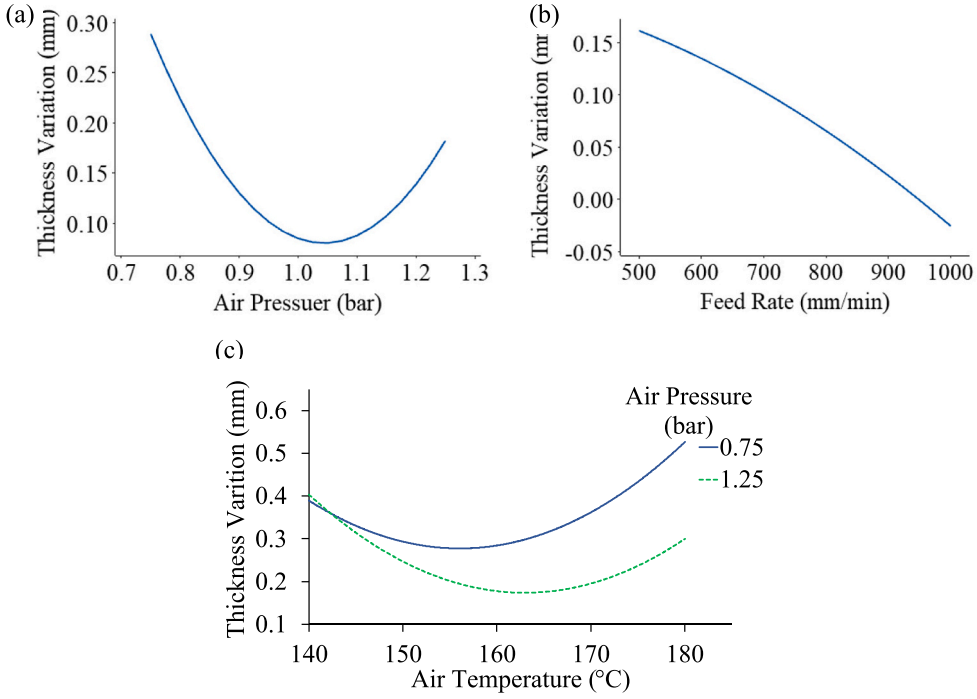

Fig. 7. Effect of (a) air pressure and (b) feed rate on thickness variation, (c) interactions among air pressure and temperature on thickness variation.

without experiencing significant degradation in their properties. This characteristic makes them highly valuable for recycling and reuse purposes [29].

Fig. 5d illustrates the relationship between feed rate and profile variation. The results exhibit a clear trend of decreasing profile variation with increasing feed rate. Specifically, the highest feed rate produced the lowest profile variation value. The reason for this effect can be explained by considering the exposure time of the localised hot air. A high feed rate reduces the exposure time, resulting in more uniform deformation. In other words, when the tool moves quickly, the hot air has less time to impact the material and cause uneven deformation. This observation aligns with previous research that has shown the critical role of exposure time in the deformation process [30]. Therefore, controlling the feed rate emerges as an important parameter to consider when optimising the deformation process and achieving a uniform profile.

In Fig. 6a, the impact of air temperature and pressure on the profile variation of a polycarbonate sheet is depicted. The two parabolic curves illustrate that both air temperature and pressure have a significant influence on the profile variation, exhibiting the same trend as in Fig. 6a.

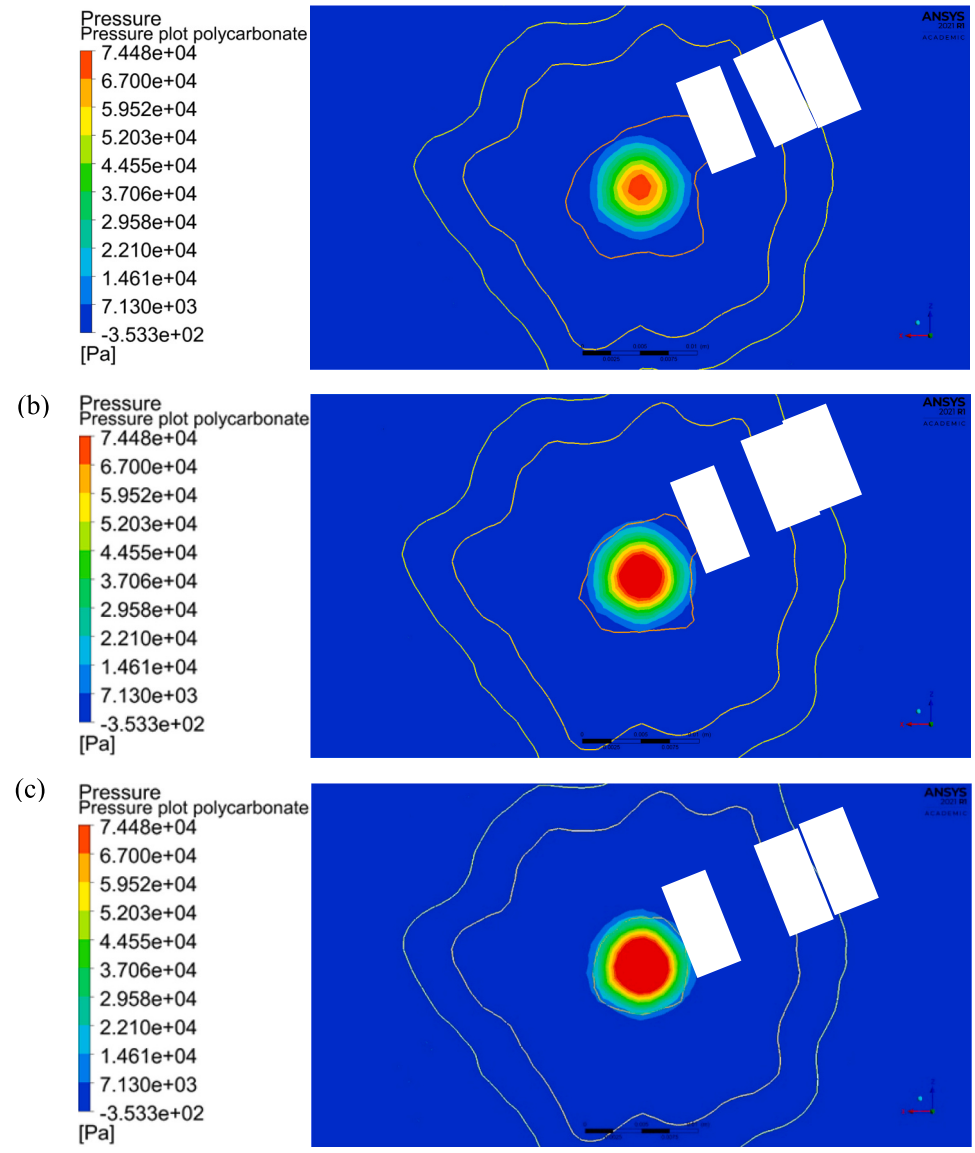

Fig. 8. CFD results of the Pressure and temperature affected area when using air pressure of (a) 0.75 bar, (b) 1 bar, and (c) 1.25 bar.

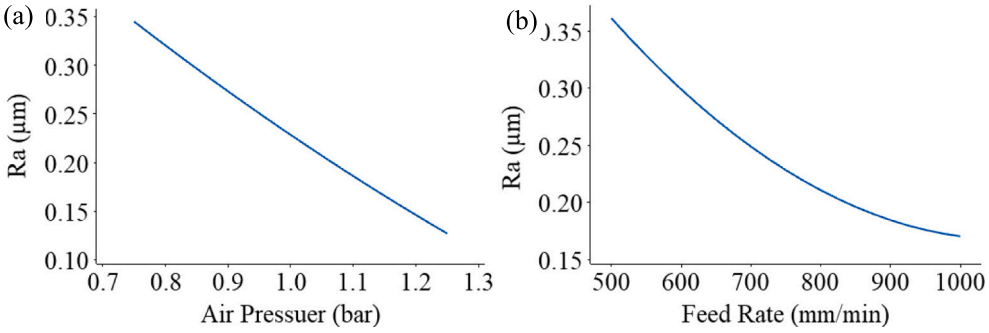

Fig. 9. Effect of (a) air pressure and (b) feed rate on surface roughness.

The figure demonstrates that the profile variation initially decreases with increasing temperature up to a certain temperature point, beyond which it starts to increase due to the material becoming too malleable [31]. At low temperatures, the highest profile variation is recorded for both air pressures, while at high temperatures, the sheet is deformed more than the target profile, resulting in over-deformation.

Additionally, the figure shows that air pressure plays a crucial role in achieving the desired profile variation of the sheet. At an air pressure of 0.75 bar, the parabolic curve has a minimum value at an air temperature of about 160 °C. Conversely, at an air pressure of 1.25 bar, the bottom of the parabolic curve shifts to the right to around 165 °C, producing the lowest profile variation of 2.4 mm. Pressures below 1 bar will not be

Table 5
Corresponding coefficient values for the prediction model.

	Profile variations	Thickness variations	Surface roughness
Constant (X)	122.2	10.61	20.11
X1	27.1	3.46	0.96
X2	1.429	0.1185	0.2435
X3	0.0090	0.00091	0.00133
X4	2.87	0.251	0.161
X5	14.2	1.46	1.56
X6	0.0455	0.01192	0.00286
X7	0.00135	0.000459	0.000768
X8	0.330	0.0228	0.0773
X9	1.26	0.177	0.394
X10	0.000058	0.000000	0.000003
X11	0.00101	0.000658	0.000199
X12	0.0137	0.00331	0.00362
X13	0.000303	0.000041	0.000011
X14	0.00564	0.000390	0.000215
X15	0.045	0.0755	0.0998
X16	16.8	2.40	0.12
X17	0.004355	0.000429	0.000748
X18	0.000004	0.000000	0.000001
X19	0.2153	0.0220	0.0119
X20	15.16	1.04	0.24

Table 6
Optimum operational parameters.

	Air pressure (bar)	Air temperature (°C)	Feed rate (mm/min)	Tool offset (mm)	Step down (mm)
Optimal parameters	1.02273	160.606	1000	8	1

sufficient to deform the sheet uniformly to the designed depth, while pressures above 1 bar will deform the sheet more than required. Therefore, controlling the air pressure within a specific range is essential for achieving the desired profile variation of the polycarbonate sheet.

Fig. 6b demonstrates the effect of air temperature and feed rate interactions on profile variation. Similar to Fig. 6a, two parabolic curves illustrate that both air temperature and feed rate have a significant influence on the profile variation. As mentioned earlier, the highest feed rate results in the lowest profile variation due to its effect on the heating, depending on the heating time. Conversely, a low feed rate produces higher profile variations, as observed with a feed rate of 500 mm/min. Higher profile variation values for all different feed rates are noted at 140 °C because the value of the storage modulus is too high to reach the softening temperature. On the other hand, the high temperature of 180 °C leads to more deformation than the designed one due to rubbery flow, causing an increase in the profile variation for all different feed rates. Consequently, the lowest profile variation is observed at transition temperature and high feed rate.

Fig. 6c. assesses the impact of the interaction between feed rate and step-down on profile variation. At a step-down of 1 mm, the profile remains almost consistent, with only a slight change in profile variation (0.495 mm ± 0.005) observed across a range of feed rates. More uniform variation is recorded at high-speed movements. In contrast, at a step-down of 0.5 mm, a sharp drop in profile variation is observed with increasing feed rate. The difference in profile between high feed rates of 1000 mm/min and low feed rates of 500 mm/min is attributed to different exposure times and surface heating, as illustrated in Fig. 6c. At low feed rates, more heat is generated for all step downs, leading to an increase in the gap between the nozzle and the sheet surface. A higher surface temperature also results in more deformation. In contrast, a high feed rate generates less heat for all step downs, and a step-down of 1 mm is the optimum value that maintains the gap similar to the end of the process and yields a more uniform profile result than a low feed rate due to exposure time. A step-down of 1 mm provides a more homogeneous profile for different feed rates than a step-down of 0.5 mm.

3.3. Thickness variation

In Fig. 7a, it is evident that air pressure has a significant influence on thickness variation. The graph exhibits a parabolic shape, indicating the presence of an optimal air pressure range for achieving uniform thickness. At low air pressure levels, such as 0.75 bar, the sheet is not uniformly deformed, resulting in high thickness variation. As the air pressure increases from 0.75 bar to 1 bar, the thickness variation decreases significantly. However, further increasing the pressure to 1.1–1.25 bar leads to an increase in thickness variation again, as the sheet is excessively deformed. The optimum air pressure value for achieving uniform thickness is found to be 1.05 bar. This suggests that careful selection and adjustment of air pressure during the process can result in more consistent and accurate thickness of the polycarbonate sheet.

Fig. 7b illustrates the effect of feed rate on thickness variation. Increasing the feed rate from 500 mm/min to 1000 mm/min results in a significant and uniform reduction in thickness variation. This is because a high feed rate (high moving speed) reduces the exposure time of localised hot air, leading to less material expansion and a decrease in thickness variation. On the other hand, a low moving speed for the nozzle provides more exposure time for heating the polycarbonate sheet, leading to an increase in thickness variation, as the amount of expansion is typically proportional to the temperature increase.

Fig. 7c showcases the impact of air temperature and pressure interactions on thickness changes. At a pressure of 0.75 bar, lower thickness variation is observed at lower temperatures, and the variation increases with increasing temperature. At low air temperatures, the effect of the air pressure is completely diminished, as the material is difficult to deform regardless of the applied air pressure up to 1.25 bar. As the temperature increases, the effect of the air pressure becomes more notable, and differences in thickness variation grow. Conversely, the differences in thickness at a pressure of 1.25 bar seem to be more consistent at lower and higher temperatures, but the best uniformity was observed at the storage modulus temperature, where the difference was less than 0.2 mm at temperature of around 160 °C. These variations in thickness are caused by the interplay between the distributions of pressure and temperature on the polycarbonate sheet.

The CFD results presented in Fig. 8 demonstrate the impact of different air pressures on the pressurised hot air jet from the contactless SPIF nozzle to the polycarbonate sheet. The results reveal that the pressure and temperature affected areas are influenced differently by varying air pressures. In Fig. 8a, the pressure-affected area is observed to be smaller than the temperature affected area by approximately two times, and the maximum pressure value recorded is 7.448×10^4 pa. In contrast, the temperature-affected area appears irregular in shape, suggesting a non-uniform heating distribution across the sheet. When the air pressure is increased to 1 bar, as shown in Fig. 8b, the pressure-affected area becomes larger, resulting in a more uniform temperature-affected area. However, it remains smaller than the temperature-affected area. This implies that increasing the air pressure can lead to a more uniform distribution of deformation on the material but does not necessarily result in a more uniform heating distribution.

Interestingly, the distribution of the pressure and temperature-

Table 7
Predicted and experimental results using the optimal conditions.

	Profile variation (mm)	Thickness variation (mm)	Surface roughness (Ra) μm
Predicted	0.971	0.133	0.068
Optimised experiment	0.996	0.14847	0.1310

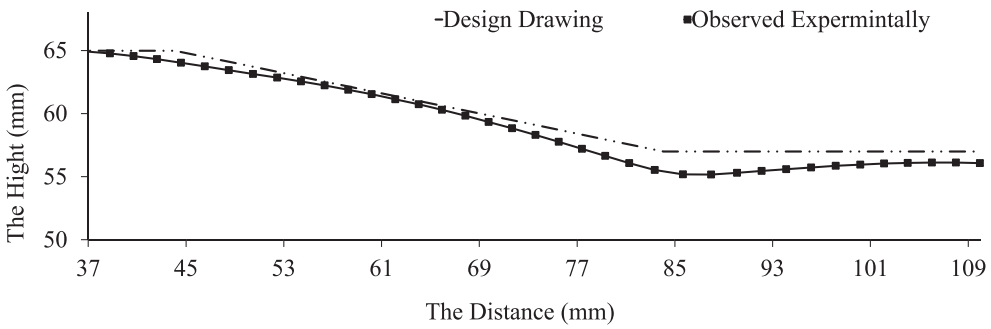

Fig. 10. Comparison between CAD drawing and experimental profile.

affected areas becomes almost equal when the air pressure is increased to 1.25 bar, as shown in Fig. 8c. This suggests that using an air pressure of 1.25 bar can result in a more uniform deformation of the material, leading to a more uniform thickness distribution, which aligns with the DOE results shown in Fig. 8c.

3.4. Surface roughness

In sheet forming processes such as in single point incremental forming, surface roughness is a crucial factor that affects the quality of the formed part. Fig. 9 demonstrates the effects of air pressure and feed rate on the surface roughness (Ra) of the formed polycarbonate sheet.

Fig. 9a shows a clear relationship between air pressure and surface roughness. It is evident that the surface roughness value decreases linearly with an increase in air pressure. This finding is consistent with observations made in conventional SPIF, where an increase in the tool tip radius led to a decrease in surface roughness [32]. The reason behind this is that the area affected by air pressure in contactless SPIF behaves similarly to the tool tip area in conventional SPIF, and an increase in air pressure leads to a decrease in surface roughness. The smoothest surface is achieved at the highest air pressure (1.25 bar), with a surface roughness value of 0.12 μm. On the other hand, when the air pressure is low (0.75 bar), the surface roughness value is high (0.35 μm).

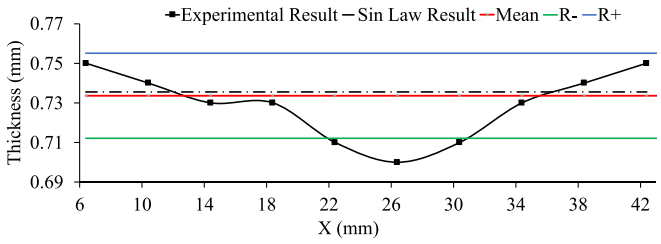

Fig. 11. Comparison of thickness distribution obtained by the theoretical sine law, and experiment.

Fig. 9b shows that increasing the feed rate results in a decrease in surface roughness. As the feed rate increases from 500 mm/min to 1000 mm/min, the surface roughness value decreases from 0.35 μm to 0.17 μm. The lowest surface roughness value is achieved at a feed rate of 1000 mm/min, while the highest surface roughness value is obtained at a lower feed rate (500 mm/min). The reason behind this is related to the effect of the heat spot generated by the nozzle on the material. At lower feed rates, the nozzle moves at a slower speed, allowing more exposure time for heating the material. This leads to deeper deformation for each path and, consequently, a higher surface roughness value. On the other hand, increasing the feed rate reduces the time of exposure to the heat spot, resulting in shallower deformation and, therefore, a lower surface roughness value.

3.5. Model predictions and process optimisation

To achieve high-quality manufacturing processes, it is essential to have a reliable model that can accurately predict the quality criteria for various combinations of process parameters. An empirical model is particularly useful in this regard, as it offers several advantages. Firstly, it provides a comprehensive understanding of how each process parameter impacts the quality criteria. Secondly, it facilitates the identification of the optimal parameters that produce the desired quality criteria. Thirdly, it can be used to optimise the manufacturing process by predicting the quality criteria for any combination of parameters. Lastly, it can reduce the need for costly and time-consuming experimental trials.

In this study, data obtained from the Design of Experiments (DOE) was used to develop an empirical model capable to describing and predicting the quality criteria of deformed polycarbonate for any combination of process parameters. The model employed a general second-order polynomial equation that incorporated the critical parameters and their interactions. Eq. (2) illustrates that each process parameter and

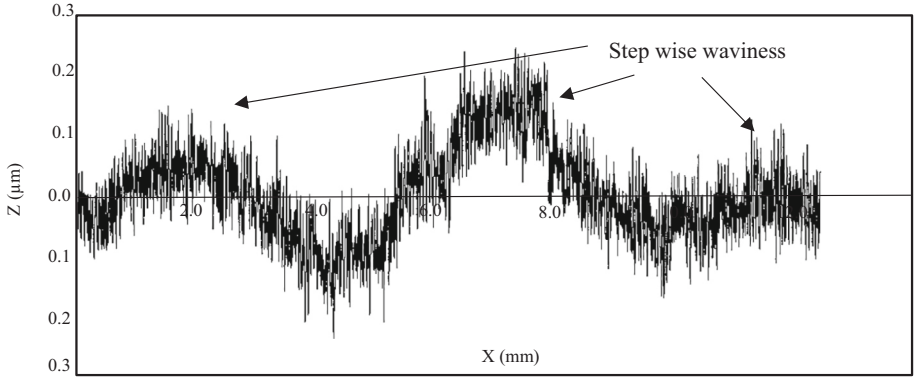

Fig. 12. Surface roughness (Ra) for samples using the optimised data.

interaction is multiplied by a coefficient. The coefficients for each process parameter and interaction were determined from the data and are presented in Table 5. The R-square value of the empirical model's exceeded 95 % for all models, indicating a strong fit. Consequently, the empirical model can accurately predict the quality criteria of deformed polycarbonate for any combination of process parameters, reducing the need for expensive and time-consuming experimental trials while optimising the manufacturing process.

$$\begin{aligned}\text{Prediction model} = {} & X - X1A - X2B - X3C + X4D + X5E - X6AB + X7AC \\ & - X8AD + X9AE + X10BC + X11BD + X12BE \\ & - X13CD + X14CE + X15DE + X16A\hat{}2 + X17B\hat{}2 \\ & - X18C\hat{}2 - X19D\hat{}2 - X20E\hat{}2 \end{aligned} \quad (2)$$

where A is the air pressure, B is the air temperature, C is the feed rate, D is the tool offset, E is the step-down, and x1 through x20 are the coefficients from Table 5.

To achieve a final product with high precision and a desirable surface finish, it is crucial to identify the optimal operational parameters. This study aims to achieve minimal deviation in profile, thickness, and surface roughness while avoiding the formation of wrinkles or severe thin spots. All parameters are limited to pre-selected levels, and each quality attribute is given equal importance. To determine the optimal parameters satisfying all the objective functions, a Min-Max optimisation method is employed, as outlined in Table 6. This method concurrently solves the three empirical equations for profile, thickness variations, and surface roughness until the working variable values meet all objective functions. The optimisation process minimises the maximum deviation from the desired values for each quality attribute, ensuring that the final product adheres the required standards.

The process parameters used were an air pressure of 1.02 bar, an air temperature of 160.60 °C, a feed rate of 1000 mm/min, a tool offset of 8 mm, and a stepdown of 1 mm. These parameters can be employed to ensure consistent and high-quality products in future manufacturing processes. Furthermore, the optimisation process aids in minimising waste and reducing costs by ensuring that the production process is optimised to achieve the desired quality standards while conserving resources.

To validate the effectiveness of the contactless SPIF technique, an experimental trial was conducted using the optimal working parameters identified during the development phase. The results demonstrated that the formed part exhibited minimal wrinkling or thinning, affirming the suitability of the process parameters for the intended application. Table 7 summarises the quality characteristics that were tested and compares them to the predictions made using the DOE. The geometric accuracy between the design and experimental results was found to be in excellent agreement, with a profile variation of only 0.996 mm. Fig. 10 illustrates this agreement, displaying the CAD profile of the manufactured workpiece alongside the experimentally measured profile under optimal operational conditions.

However, the comparison of thickness between the measured experimental results and the theoretical sine law values using the optimal parameters revealed a small but acceptable difference, see Fig. 11. This discrepancy can be attributed to the inherent complexities of the process and the uncertainties present in the actual manufacturing environment. Furthermore, the surface roughness (Ra) results for samples prepared using the optimised process parameters differed significantly from the predicted values. Subsequent analysis revealed that the waviness on the formed sheet was due to the step-down phenomenon of the process, leading to an increase in roughness. Fig. 12 visually illustrates this phenomenon. In summary, the experimental trial confirmed the effectiveness of the contactless SPIF technique, highlighting its potential while also emphasising the need for further optimisation to achieve the desired surface finish.

4. Conclusion

This study introduces and optimises a highly flexible and adaptable contactless SPIF process utilizing hot pressurised air as the forming tool to meet diverse manufacturing demands and customer requirements. By eliminating the interaction between the forming tool and the sample, the contactless SPIF process offers several benefits, including reduced tool wear, enhanced design flexibility, and improved dimensional accuracy.

To assess the process's effectiveness, 54 different forming conditions were tested and analysed using the Design of Experiments (DOE) methodology and a response surface method to pinpoint the most significant process variables. The study revealed that air pressure, air temperature, and feed rate were the most critical variables influencing the formability of the process, while the tool offset had no discernible effect. Significant parameter interactions were identified for profile variation, thickness variation, and surface roughness, and a mathematical model was developed to characterise the influence of the process components.

Researchers found that increasing the feed rate reduced profile variation, thickness variation, and surface roughness, while increasing air pressure had a opposite effect. By employing the min-max approach to optimisation, they pinpointed process parameters values that struck an optimal balance among conflicting quality characteristics. The optimised experiment in this study demonstrated that the contactless SPIF process can be tailored for a wide range of polymer materials. It produced a truncated pyramid polycarbonate shape with exceptional accuracy and consistency by identifying the key variables and optimising their settings. This finding is particularly significant considering the increasing demand for high-quality, complex-shaped plastic components in various industries, including automotive, aerospace, and consumer goods.

Ethical approval

The authors confirm that this work does not contain any studies with human participants performed by any of the authors.

Funding

No funding is applicable.

Declaration of competing interest

The authors of this article declare that they have no conflicts of interest regarding the publication of this manuscript.

Data availability

All data generated or analysed during this study are included in this published article.

References

[1] Radu C. Effects of process parameters on the quality of parts processed by single point incremental forming. Int J Mod Manuf Technol 2011;3(2):91–6.
[2] Petek A, Kuzman K, Kopač J. Deformations and forces analysis of single point incremental sheet metal forming. Archives of Materials science and Engineering 2009;35(3):107–16.
[3] Abaas TF, Bedan AS. The effect of tool path strategy on mechanical properties of Brass (65-35) in single point incremental sheet metal forming (SPIF). Journal of Engineering 2013;19(5).
[4] Kim Y, Park J. Effect of process parameters on formability in incremental forming of sheet metal. J Mater Process Technol 2002;130:42–6.
[5] Azevedo NG, et al. Lubrication aspects during single point incremental forming for steel and aluminum materials. International Journal of precision engineering and manufacturing 2015;16(3):589–95.
[6] Durante M, Formisano A, Lambiase F. Incremental forming of polycarbonate sheets. J Mater Process Technol 2018;253:57–63.
[7] Rosa-Sainz A, et al. Experimental failure analysis in polycarbonate sheet deformed by spif. Journal of Manufacturing Processes 2021;64:1153–68.

[8] Martins PAF, et al. Single point incremental forming of polymers. CIRP Annals 2009;58(1):229–32.
[9] Yan Z, Hassanin H, El-Sayed MA, Eldessouky HM, Djuansjah J, Alsaleh NA, Essa K, Ahmadein M. Multistage Tool Path Optimisation of Single-Point Incremental Forming Process. Materials 2021;14:6794. https://doi.org/10.3390/ma14226794.
[10] Essa K, Hartley P. Optimization of conventional spinning process parameters by means of numerical simulation and statistical analysis. Proceedings of the Institution of Mechanical Engineers, Part B: Journal of Engineering Manufacture 2010;224(11):1691–705.
[11] Majagi SD, Chandramohan G. Optimization of incremental sheet metal forming parameters by design of experiments. In: Applied mechanics and materials. Trans Tech Publ; 2014.
[12] Le VS, Ghiotti A, Lucchetta G. Preliminary studies on single point incremental forming for thermoplastic materials. International Journal of Material Forming 2008;1(1):1179–82.
[13] Jurisevic B, Kuzman K, Junkar M. Water jetting technology: an alternative in incremental sheet metal forming. The International Journal of Advanced Manufacturing Technology 2006;31(1–2):18–23.
[14] Jurisevic, B., et al. *Incremental sheet metal forming process with a water jet and rigid tool.* in *Proc 17th International Conference on Water Jetting.* 2004.
[15] Yang C, Sheu S, Yu K. Optimal machining parameters in the cutting process of glass fibre using the reliability analysis based on the Taguchi method. Proceedings of the Institution of Mechanical Engineers, Part B: Journal of Engineering Manufacture 2008;222(9):1075–82.
[16] Bacchewar P, Singhal S, Pandey P. Statistical modelling and optimization of surface roughness in the selective laser sintering process. Proceedings of the Institution of Mechanical Engineers, Part B: Journal of Engineering Manufacture 2007;221(1):35–52.
[17] Hussain G, Gao L, Hayat N. Empirical modelling of the influence of operating parameters on the spifability of a titanium sheet using response surface methodology. Proceedings of the Institution of Mechanical Engineers, Part B: Journal of Engineering Manufacture 2009;223(1):73–81.
[18] Ham M, Jeswiet J. Forming limit curves in single point incremental forming. CIRP annals 2007;56(1):277–80.
[19] Filice L, Ambrogio G, Micari F. On-line control of single point incremental forming operations through punch force monitoring. CIRP annals 2006;55(1):245–8.
[20] Ham M, Jeswiet J. Single point incremental forming and the forming criteria for AA3003. CIRP annals 2006;55(1):241–4.
[21] Ambrogio G, et al. An analytical model for improving precision in single point incremental forming. J Mater Process Technol 2007;191(1–3):92–5.
[22] Elghawail A, et al. Prediction of springback in multi-point forming. Cogent Engineering 2017;4(1):1400507.
[23] Cao K, Wang Y, Wang Y. Experimental investigation and modeling of the tension behavior of polycarbonate with temperature effects from low to high strain rates. International Journal of Solids and Structures 2014;51(13):2539–48.
[24] Li Y, et al. Effects of process parameters on thickness thinning and mechanical properties of the formed parts in incremental sheet forming. The International Journal of Advanced Manufacturing Technology 2018;98:3071–80.
[25] Abosaf M, et al. Optimisation of multi-point forming process parameters. The International Journal of Advanced Manufacturing Technology 2017;92:1849–59.
[26] Siviour, C., et al., *Mechanical behaviour of polymers at high rates of strain.* https://doi.org/10.1051/jp4:2006134145, 2006. 134.
[27] Sehrawat M, et al. Glass transition temperature measurement of polycarbonate specimen by dynamic mechanical Analyser towards the development of reference material. MAPAN 2022;37(3):517–27.
[28] Mulliken AD, Boyce MC. Mechanics of the rate-dependent elastic–plastic deformation of glassy polymers from low to high strain rates. International journal of solids and structures 2006;43(5):1331–56.
[29] Pelin C-E, et al. Recycling and reusing polyamide 6 extruded waste products to manufacture carbon fiber based composites. Annals of the Academy of Romanian Scientists Series on Physics and Chemistry Science 2017;2:91–103.
[30] Ayhan Z, Zhang Q. Wall thickness distribution in thermoformed food containers produced by a Benco aseptic packaging machine. Polymer Engineering and Science - POLYM ENG SCI 2000;40:1–10.
[31] Dunson D. Characterization of polymers using dynamic mechanical analysis (DMA). EAG Appl Note 2017:1–8.
[32] Sabater M, et al. Process parameter effects on biocompatible thermoplastic sheets produced by incremental forming. Materials 2018;11(8):1377.